Journal of Reproduction and Development, Vol. 70, No 1, 2024

Original Article

PABPN1L is required for maternal mRNA degradation after meiosis resumption

Chihiro EMORI[1)*], Mayo KODANI[1, 2)*], Ferheen ABBASI[1, 3)], Masashi MORI[1)] and Masahito IKAWA[1, 2, 4–6)]

[1)]*Research Institute for Microbial Diseases, Osaka University, Osaka 565-0871, Japan*
[2)]*Graduate School of Pharmaceutical Sciences, Osaka University, Osaka 565-0871, Japan*
[3)]*Graduate School of Medicine, Osaka University, Osaka 565-0871, Japan*
[4)]*Immunology Frontier Research Center, Osaka University, Osaka 565-0871, Japan*
[5)]*The Institute of Medical Science, The University of Tokyo, Tokyo 108-8639, Japan*
[6)]*Center for Infectious Disease Education and Research (CiDER), Osaka University, Osaka 565-0871, Japan*

Abstract. Poly(A)-binding proteins (PABPs) play roles in mRNA maturation, translational activity, and decay. The functions of PABPs, especially PABPN1 and PABPC1, in somatic cells have been well-studied. However, little is known about the roles of PABPs in oocytes because of the unique mechanisms of mRNA metabolism in oocytes. This study focused on PABPN1L and generated *Pabpn1l* knockout (KO) mice using the CRISPR/Cas9 system. After mating tests, we found that *Pabpn1l* KO females were infertile due to the failure of the embryos to develop to the 4-cell stage. RNA-seq analysis revealed aberrant mRNA persistence in *Pabpn1l* KO-MII oocytes, which indicates impaired mRNA degradation during the germinal vesicle (GV) to MII transition. We also revealed that the exogenous expression of *Pabpn1l* mRNA in KO-GV oocytes recovered defects of embryonic development. PABPN1L is partly indispensable for female fertility in mice, owing to its necessity for embryonic development, which is supported by mRNA degradation during GV to MII maturation.
Key words: Fertility, Oocyte, PABPN1L

(**J. Reprod. Dev. 70:** 10–17, 2024)

Eukaryotic pre-mRNA undergoes processing, such as 5′capping, splicing, and 3′polyadenylation, before transport from the nucleus to the cytoplasm and subsequent translation [1, 2]. Mature mRNA forms a loop structure with a protein complex, in which eukaryotic initiation factor (eIF) and poly(A)-binding protein (PABP) interact with the 5′cap and poly(A) tail, respectively [3, 4]. The resulting translation initiation complex enhances translation by increasing eIF recruitment. The functions of some PABP members in somatic cells have been well-studied. In the nucleus, PABP nuclear 1 (PABPN1) binds to nascent poly(A) tails and promotes adenylation to 200–250 nucleotides long by cooperating with poly(A) polymerase (PAP) [5]. In the cytoplasm, PABP cytoplasmic 1 (PABPC1) covers the elongated poly(A) tails and regulates mRNA metabolism by coordinating with the CCR4-NOT deadenylase complex [6,7]. mRNA metabolism is an important event in somatic and germ cells and has unique mechanisms in oocytes. During oogenesis, mRNAs are transcribed and stored in the cytoplasm, and this accumulation is completed by the fully grown germinal vesicle (GV) stage, when global transcriptional silencing occurs. The stored maternal mRNAs are utilized for the resumption of meiosis, fertilization, and early embryonic development [8,9], and are degraded when the zygotic genome starts to be transcribed after fertilization. Defects in maternal mRNA decay lead to the loss of zygotic gene activation, resulting in embryonic developmental arrest [10–13]. As members of the PABP family, PABPN1L and PABPC1L are specifically expressed in the oocytes. PABPC1L increases the poly(A) length of maternal mRNAs, such as *c-mos* or *Dazl* in oocytes, and enables the translation of these maternal transcripts [14]. Thus, female mice lacking *Pabpc1l* fail to generate mature second metaphase (MII) oocytes, resulting in infertility. *Pabpn1l* was first identified in *Xenopus* and mouse oocytes. The *Xenopus* Pabpn1l protein is expressed during oogenesis and early embryogenesis and is degraded after zygotic transcription begins [15]. Mouse *Pabpn1l* is also expressed in oocytes, and during early development, knockout females show defects in the deadenylation and degradation of maternal mRNAs [16]. However, the detailed function of PABPN1L in the GV/MII stage is not well-understood.

In this study, we used the CRISPR/Cas9 system to generate *Pabpn1l* knock out (KO) mice and confirmed that PABPN1L is indispensable for female fertility. Furthermore, mRNA complementation analysis suggests that PABPN1L is critical for mRNA degradation during the GV/MII stage, which cannot be complemented by PABPC1.

Materials and Methods

Animals and ethics

All animal experiments were approved by the Institutional Animal Care and Use Committee of the Research Institute for Microbial Diseases, Osaka University (Osaka, Japan), and were conducted in compliance with the guidelines and regulations for animal experimentation. B6D2F1 and C57BL/6 mice were purchased from CLEA Japan, Inc. (Tokyo, Japan) or Japan SLC, Inc. (Shizuoka, Japan).

Received: September 13, 2023
Accepted: November 9, 2023
Advanced Epub: December 7, 2023

Correspondence: M Ikawa (e-mail: ikawa@biken.osaka-u.ac.jp)
* C Emori and M Kodani equally contributed.

RNA purification and RT-PCR

RNA was isolated and purified from multiple adult tissues (brain, lung, liver, thymus, ovary, uterus, oviduct, testis, kidney, heart, and spleen) and oocytes using TRIzol reagent (15596018, Thermo Fisher Scientific, Waltham, MA, USA). RNA was reverse transcribed to cDNA using the SuperScript III First-Strand Synthesis System (18080051; Thermo Fisher Scientific). RT-PCR was performed using a KOD FX Neo (KFX-201; Toyobo, Osaka, Japan). The primers used for PCR are listed in Table 1. RNA used for ovary stage-specific RT-PCR was isolated and purified from mouse ovaries on postnatal days 0, 7, 14, and 21, using an RNeasy Micro Kit (QIAGEN, Hilden, Germany). GV oocytes were collected by dissecting the ovaries of the females injected with CARD HyperOva® following the manufacturer's protocol (Kyudo, Saga, Japan). Oocytes at the MII stage were collected from the oviducts of females that had been injected with CARD HyperOva®, followed 48 h later by human chorionic gonadotropin (hCG) (5 units, ASKA Pharmaceutical, Tokyo, Japan). Two-pronuclear (2PN) embryos, 2-cell embryos, 4-cell embryos, morulae, and blastocysts were collected at 8, 24, 48, 72, and 96 h after insemination. All tissues, oocytes, and embryos were collected from C57BL/6 mice.

Generation of Pabpn1l KO mice and Pabpn1l KI mice with the CRISPR/Cas9 system

Pabpn1l knockout (KO) mice (*Pabpn1l*$^{-/-}$ mice) were generated using CRISPR/Cas9 genome editing technology. Single-guide RNA (sgRNA) was designed using the web tool CRISPRdirect (https://crispr.dbcls.jp/) [17], and its cleavage efficiency was evaluated by transfecting HEK293T cells with pCAG-EGxxFP (Addgene #50716) plasmids as previously described [18]. The gRNA sequence selected for the crRNA was 5′-CAGGATCTGAGGAGACCGTC-3′. Hormonally primed B6D2F1 females were paired with wild-type males, and embryos were collected from the oviducts. pX330 plasmids expressing sgRNAs and Cas9 were microinjected into the pronuclei of zygotes as previously described [18]. Two-cell embryos were then transplanted into pseudopregnant females. Using an sgRNA targeting exon 1 (Supplementary Fig. 1A), we obtained a mouse with a 13-bp deletion in the allele (Supplementary Fig. 1B), which caused a frameshift leading to a premature stop codon (Supplementary Fig. 1C). This 13-bp deletion was detected by PCR and subsequent multiNA microchip electrophoresis (SHIMADZU, Kyoto, Japan) (Supplementary Fig. 1D). *Pabpn1l* knock-in (KI) mice (*Pabpn*$^{KI/KI}$ mice) were generated using CRISPR/Cas9 genome editing technology. Briefly, the crRNA/tracrRNA/Cas9 ribonucleoprotein complex was electroporated into wild-type zygotes with oligonucleotides carrying PA and 1D4 tags sandwiched between homology arms (50 nt on both sides) using a NEPA21 electroporator (NEPA GENE, Chiba, Japan) (Supplementary Fig. 2A). Two-cell embryos were transplanted into pregnant females. The gRNA sequence selected was 5′-GTACGGGCTAAACCATTG-3′. Genotyping PCR was performed using KOD FX Neo (KFX-201), and amplicons were observed using MultiNA. The primers used for PCR are listed in Table 1. *Pabpn1l*$^{-/-}$ mice generated and used in this study are available through the Riken BioResource Center, Ibaraki, Japan (RBRC numbers: 10821) or the Center for Animal Resources and Development (CARD), Kumamoto University, Kumamoto, Japan (CARD ID: 2801).

Fertility test

Sexually mature (7–20-week-old) *Pabpn1l*$^{-/-}$ or wild-type female mice were caged with 8-week-old male wild-type mice for 2 months. Vaginal plugs and the number of pups at birth were daily counted. The average number of pups/plugs was calculated by dividing the total number by the number of plugs.

Ovary collection and HE staining

Ovaries were dissected from *Pabpn1l*$^{+/-}$ or *Pabpn1l*$^{-/-}$ female mice (14–19-week-old), fixed in Bouin's fluid (Polysciences Inc., Warrington, PA, USA), and embedded in paraffin wax. Paraffin sections (5 μm) were stained with Mayer's hematoxylin solution (FUJIFILM Wako Pure Chemical, Osaka, Japan) and counterstained with 0.3% eosin (FUJIFILM Wako Pure Chemical). Sections were observed using phase-contrast microscopy.

In vitro fertilization (IVF)

In vitro fertilization was performed as previously described [19]. Briefly, spermatozoa were obtained from the caudal epididymis of adult WT males and cultured in TYH medium [20] for 2 h at 37°C under 5% CO_2. MII oocytes were collected from the oviducts of 8-week-old females injected with pregnant mare serum gonadotropin (PMSG) (5 units; ASKA Pharmaceutical), followed by hCG injection (5 units) 48 h later. After incubation, spermatozoa were added to a drop of cumulus-intact MII oocytes at a final density of 2×10^5 spermatozoa/ml. Eight hours after adding the spermatozoa, the 2PN embryos were moved into potassium-supplemented simplex-optimized medium (KSOM) [21] for further observation. Embryos were observed under an Olympus IX73 microscope (OLYMPUS, Tokyo, Japan) 8, 24, 48, and 96 h after insemination.

RNA sequencing analysis

GV oocytes were collected from the ovaries of 3–4-month-old female mice injected with PMSG (5 units). MII-stage oocytes were collected from the oviducts of 3–4-month-old females that had been

Table 1. Primers used for RT-PCR, genotyping, and mRNA preparation and conditions of PCR

Methods	Gene name	Forward 5′- 3′	Reverse 5′- 3′	Product size (bp)
RT-PCR	*Pabpn1l*	TTGGATCCGCCGCCATGGAGCCTTACCTGAGCAATGAGC	TTGAATTCGTAGGGAGAGAACCACTGTGGTGCT	841
RT-PCR	*Actb*	CATCCGTAAAGACCTCTATGCCAAC	ATGGAGCCACCGATCCACA	171
Genotyping (WT)	*Pabpn1l*	TCCGGCTGGGCTTCAGCATG	GAAGCCTGGCTCCAGATCCT	556
Genotyping (KO)	*Pabpn1l*	TCCGGCTGGGCTTCAGCATG	CTCCAGACGGTCTCCTCAGA	560
mRNA preparation	*Pabpn1l*	GGGTAATACGACTCACTATAGGGGCAACGTGCTGGTTGTTGTGC	AGCCAGAAGTCAGATGCTCAAGGGGCTTC	–

injected with PMSG (5 units) and hCG (5 units). Total RNA of GV or MII oocytes from *Pabpn1l*$^{+/-}$ or *Pabpn1l*$^{-/-}$ mice were extracted using the SMART-seq v4 Ultra Low Input RNA Kit for sequencing (Takara Bio USA, Inc., Mountain View, CA, USA). The resulting libraries were sequenced using the HiSeq 2500 system (Illumina, San Diego, CA, USA). Genes with fragments per kilobase of transcript per million reads mapped (FPKM) < 1 were excluded from subsequent analysis. The RNA sequencing data were deposited in the Sequence Read Archive (temporary submission ID: PSUB021157), https://www.ddbj.nig.ac.jp/dra/index-e.html).

Poly(A) length analysis

The poly(A) length dataset in GV-stage oocytes was downloaded from a paper published by Morgan *et al.* [22]. The transcripts expressed at the GV stage were counted according to the poly(A) length and divided by the total number of transcripts in GV oocytes (total transcripts: 12,411). Data from Morgan *et al.* and our RNA-seq data were compared, and the transcripts degraded in the presence or absence of PABPN1L were counted and divided by the total number of transcripts.

mRNA preparation for microinjection

PA-1D4 tagged-*Pabpn1l* cDNA or EGFP cDNA with a rabbit poly(A) signal was constructed for mRNA synthesis (Supplementary Figs. 3A, 3B). *Pabpn1l* and EGFP sequences were amplified by PCR using primers containing the T7 promoter and a reverse primer containing the poly(A) signal sequence (Table 1). The amplicons were then transcribed into mRNA using the mMESSAGE mMACHINE T7 Transcription Kit (Thermo Fisher Scientific). After DNase treatment, a poly(A) tail was added using a Poly(A) Tailing Kit (Thermo Fisher Scientific). The mRNAs were diluted to 50 ng/µl before use.

mRNA injection

Fertilized embryos at the 2PN stage were collected from the oviducts of PMSG/hCG-primed *Pabpn1l*$^{-/-}$ and wild-type females caged with B6D2F1 males. *Pabpn1l* mRNAs and EGFP mRNAs (final concentration for each: 50 ng/µl) were mixed and injected using a piezo-micromanipulator (Prime Tech, Ibaraki, Japan) in Hepes-CZB medium. After injection, the embryos were transferred to KSOM for further culture and continuously observed until the blastocyst stage. GV oocytes were harvested from PMSG-primed *Pabpn1l*$^{-/-}$ or wild-type ovaries. *Pabpn1l* mRNAs were co-injected with EGFP mRNAs using a FemtoJet 4i microinjector (Eppendorf, Hamburg, Germany). To prevent GV breakdown, milrinone (final concentration: 10 µM) (Sigma-Aldrich, St. Louis, MO, USA) was supplemented in the medium. One hour after injection, oocytes were transferred into the αMEM medium (Sigma-Aldrich) containing 5% fetal bovine serum (FBS) (Biowest, Nuaillé, France), 25 µg/ml sodium pyruvate (Nacalai, Kyoto, Japan), 0.1 U/ml follicle-stimulating hormone (FSH), 4 ng/ml epidermal growth factor (EGF) (R&D systems, Minneapolis, MN, USA), and 1.2 IU/ml gonadotropin to mature oocytes [23]. Fourteen hours after *in vitro* maturation, mature MII oocytes were transferred to Human Tubal Fluid (HTF) medium and inseminated with spermatozoa, which were preincubated for 1 h. Embryos fertilized with 2PN were transferred to KSOM for further *in vitro* culture. Oocytes and embryos with GFP signals were observed using a Keyence BZ-X710 microscope (Keyence, Osaka, Japan) at the MII stage and at 8, 24, 48, 72, and 96 h after insemination.

Statistical analysis

Statistical analyses were performed using the Student's *t*-test (two-tailed). Data are represented as the mean ± standard deviation (SD), and error bars indicate SD.

Results

PABPN1L is expressed in oocytes and embryos

To determine the tissues that expressed *Pabpn1l* mRNA, we performed RT-PCR on various tissues and oocytes obtained from adult mice. Although weak signals were observed in the thymus, ovaries, and testes, a strong signal was detected in the oocytes, indicating that *Pabpn1l* mRNA was abundant in the ovaries (Fig. 1A). Next, we conducted RT-PCR using cDNA obtained from postnatal ovaries (postnatal days P0, 7, 14, and 21) and detected a single band at P7,

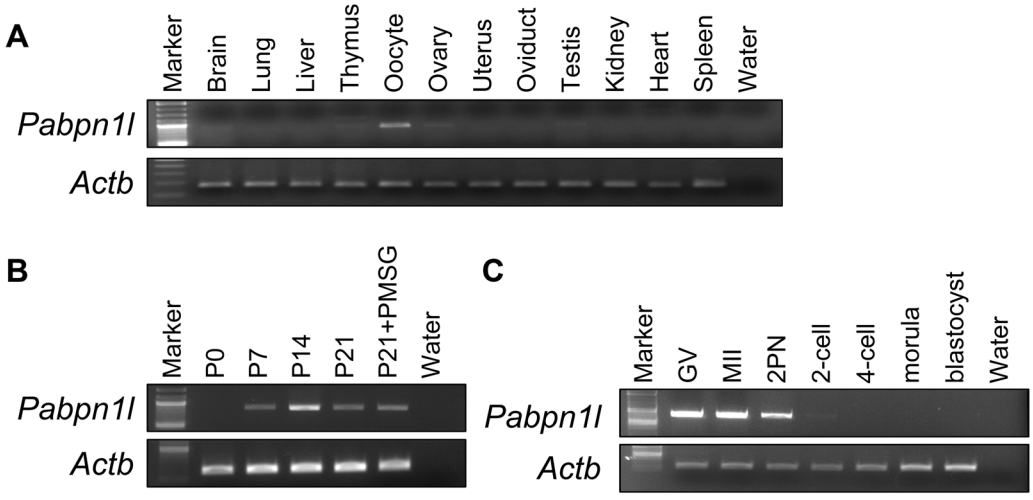

Fig. 1. Expression of mouse *Pabpn1l* mRNA. (A) RT-PCR analysis using multiple tissues. *Pabpn1l* was expressed in the ovary and oocyte. Actin beta (*Actb*) was used as an internal control. (B) RT-PCR analysis using ovaries at different ages. *Pabpn1l* starts to be expressed in the ovary at postnatal day 7. *Actb* was used as an internal control. (C) RT-PCR using oocytes and zygotes at different stages. Expression of mouse *Pabpn1l* was examined by RT-PCR using GV oocytes, MII oocytes, two-pronuclear (2PN) embryos, 2-cell embryos, 4-cell embryos, morulae, and blastocysts. *Actb* was used as an internal control.

suggesting that *Pabpn1l* mRNA is expressed around the primary follicle stage (Fig. 1B). The peak signal was observed at P14 and then decreased, possibly due to the proliferation of somatic cells in the ovary. The RT-PCR of oocytes and embryos revealed signals at the GV, MII, and 2PN stages (Fig. 1C). No signals were observed after the 2-cell stage. Considering all the RT-PCR data shown in Fig. 1, *Pabpn1l* mRNA was continuously expressed in primary follicle oocytes and degraded after fertilization.

To examine the PABPN1L protein levels in oocytes and embryos, we generated a rabbit antibody against PABPN1L, which was non-functional for either western blotting or immunofluorescence. Therefore, we generated knock-in (KI) mice expressing PA and 1D4 tags at the C-terminus of the endogenous *Pabpn1l* gene using the CRISPR/Cas9 system (Supplementary Fig. 2A). The tagged-PABPN1L proteins first appeared in MII oocytes, peaked in 2PN embryos, and disappeared in 2-cell embryos (Supplementary Fig. 2B), indicating that PABPN1L functions during fertilization. This observation is consistent with the results of a previous study [16].

PABPN1L is required for female fertility and post-fertilization development

To elucidate the physiological function of PABPN1L, we generated *Pabpn1l* KO mice using the CRISPR/Cas9 system. *Pabpn1l*$^{-/-}$ mice appeared normal and developed until term. To analyze the fertility of *Pabpn1l*$^{-/-}$ female mice, individual wild-type or *Pabpn1l*$^{-/-}$ females were caged with wild-type males and checked for mating plugs and the presence of newborn pups for two months. Control mice produced an average of 9.3 pups per plug, whereas *Pabpn1l*$^{-/-}$ females never delivered pups despite frequent plugs (Fig. 2A). *Pabpn1l*$^{-/-}$ males were fully fertile. To determine the cause of infertility, ovarian histology and oocyte formation were examined. Ovarian histology showed that all follicular stages were present in *Pabpn1l*$^{-/-}$ ovaries without any apparent abnormalities (Fig. 2B). Hormone-primed *Pabpn1l*$^{-/-}$ females ovulated a comparable number of oocytes to that of control females (average number of oocytes ovulated: 37.8 ± 19.0 from control and 31.8 ± 3.8 from *Pabpn1l*$^{-/-}$, $P > 0.05$.) (Supplementary Table 2), suggesting that the direct cause of infertility occurs after ovulation.

We then conducted *in vitro* fertilization and observed that the *Pabpn1l* KO oocytes, which were morphologically normal, were fertilized at rates similar to those of the wild-type control (Supplementary Table 1). However, zygotes derived from KO oocytes stopped developing at the 2PN or 2-cell stages (Supplementary Figs. 2C, 2D). This developmental defect was also observed *in vivo*. *Pabpn1l*$^{+/-}$ and *Pabpn1l*$^{-/-}$ females were hormonally primed and caged with wild-type males. Fifty-two hours after hCG injection, 4-cell embryos were collected from the oviducts of *Pabpn1l*$^{+/-}$ females, but not from *Pabpn1l*$^{-/-}$ females (Supplementary Fig. 4).

Taken together, we conclude that *Pabpn1l* is a maternal-effect gene, and that its disruption arrests embryonic development.

PABPN1L is involved in mRNA degradation

Impaired maternal mRNA clearance during oocyte and embryo maturation prevents zygotic genome activation and early embryonic development [12, 13]. Therefore, we conducted RNA sequencing of GV and MII oocytes when mRNA transcription ceased in maturing oocytes. The scatter plot showed that although only a few genes showed differences (fold change (FC) > 2) at the GV stage, many transcripts in KO-MII oocytes showed higher expression levels (FC > 2) than those in Het-MII oocytes (Fig. 3A). These results indicate that PABPN1L accelerates mRNA degradation during the GV/MII transition.

Poly(A) length at the GV stage does not affect mRNA degradation

When transcripts degraded during the GV/MII transition (FC > 2) were compared, 1,301 of 1,816 genes were represented in both Het and KO oocytes (Fig. 3B), suggesting that these transcripts were degraded regardless of PABPN1L. In contrast, transcripts from the remaining 515 genes were degraded by PABPN1L. To elucidate the mechanism of PABPN1L dependency, we focused on the length of the poly(A) tails of the mRNA. However, both PABPN1L-dependent and -independent degraded transcripts tended to have a peak poly(A) length of approximately 70 nucleotides (Fig. 3C). This tendency was consistent with that observed for all transcripts expressed in GV oocytes. Thus, we concluded that the poly(A) length in GV-stage oocytes does not affect their degradation efficiency via PABPN1L.

Exogenous expression of Pabpn1l in GV oocytes rescues the developmental defects in KO oocytes.

To investigate when PABPN1L functions, we injected *Pabpn1l* mRNA into KO oocytes before or after fertilization and observed their development (Fig. 4A). EGFP mRNA was used as an injection control. When we injected mRNAs into 2PN embryos derived from KO oocytes fertilized with WT sperm; these embryos developed to 4-cell at 18 ± 13% and blastocyst at 0% (Fig. 4B). Next, we injected the mRNAs into KO-GV oocytes, performed *in vitro* maturation, and fertilized them with WT sperm (Fig. 4A). Two-pronuclear embryos injected with mRNAs at GV stage developed to 4-cell stage and blastocyst (4-cell rate 84 ± 14% in injected WT oocytes, 59 ± 7% in injected KO oocytes, blastocyst rate 71 ± 26% in injected WT oocytes, 28 ± 19% in injected KO oocytes) (Fig. 4C). These data support the hypothesis that PABPN1L functions during the GV–MII transition. Restoration of the developmental ability of *Pabpn1l* KO oocytes confirms that the infertility phenotype in *Pabpn1l*$^{-/-}$ mice was caused by the loss of *Pabpn1l*. Since both PABPC1 and PABPN1L are known to mediate mRNA decay via the CNOT complex [7, 16], we examined whether PABPN1L function was compensated by PABPC1 by injecting *Pabpc1* mRNA into KO-GV oocytes and observing their development. Although the control oocytes developed to 4-cell and blastocyst at a high ratio (4-cell rate 92 ± 11% in injected WT oocytes, blastocyst rate 75 ± 18% in injected WT oocytes), the KO oocytes with *Pabpc1* injected rarely developed to either 4-cell or blastocyst (4-cell rate 2 ± 2% in injected KO oocytes, blastocyst rate 2 ± 2% in injected KO oocytes) (Supplementary Fig. 5). This indicates that the recruitment of the CNOT complex in oocytes requires PABPN1L to be uniquely expressed in oocytes and enables the further development of embryos.

Discussion

Pabpn1 and *Pabpc1* are expressed in somatic cells. However, *Pabpn1l* and *Pabpc1l* are specifically expressed in oocytes. The knockout of *Pabpn1l* results in female infertility [16]. In this study, we generated *Pabpn1l* KO mice using the CRISPR/Cas9 system and confirmed that *Pabpn1l* KO females were infertile due to the aberrant mRNA degradation observed in the *Pabpn1l* KO-MII oocytes. A previous study showed differences in mRNA expression between GV oocytes and zygotes. However, we showed that differences in mRNA expression were already observed in MII stage oocytes, and we partly rescued its function by mRNA injection at the GV stage, but not in zygotes. Our study specified the timing of function PABPN1L because existence of PABPN1L from the GV stage to zygotes rescued its KO phenotype.

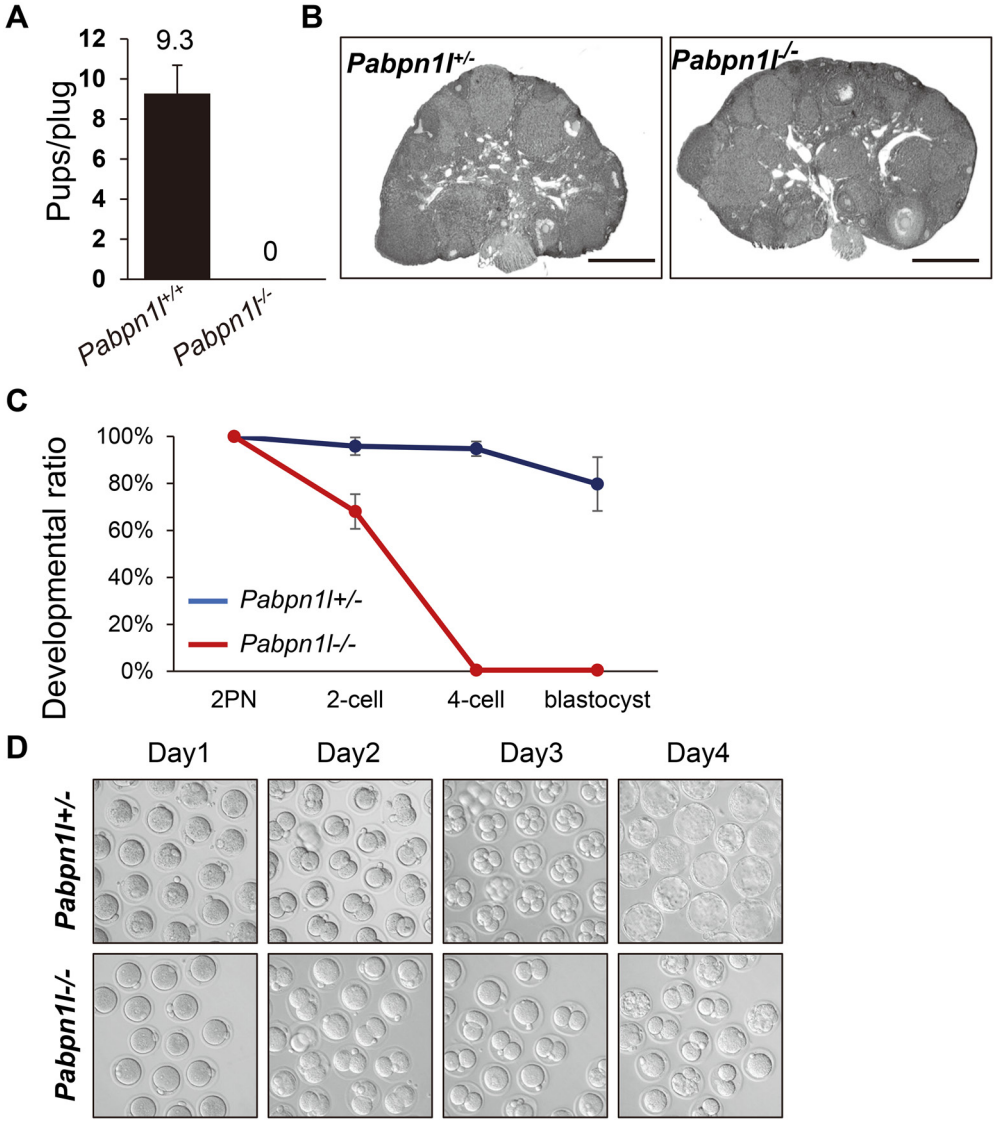

Fig. 2. The phenotypic analysis of *Pabpn1l*$^{-/-}$ females. (A) Average number of pups per plugs of wild-type and *Pabpn1l*$^{-/-}$ females. Eight *Pabpn1l*$^{-/-}$ females were examined. Wild-type females were employed as controls. (B) Morphology of the ovaries in *Pabpn1l*$^{+/-}$ and *Pabpn1l*$^{-/-}$ females. Morphology of the ovaries from three *Pabpn1l*$^{-/-}$ were observed. Ovaries from *Pabpn1l*$^{+/-}$ females were considered as controls. Scale bar: 500 µm. (C) Developmental ratio of the embryos after *in vitro* fertilization. Embryos were observed 8, 24, 48, and 96 h after insemination to detect the development to 2PN embryos, 2-cell embryos, 4-cell embryos, and blastocysts, respectively. The number of embryos at each stage was divided by the number of 2PN embryos. Embryos derived from four *Pabpn1l*$^{+/-}$ females (control) and four *Pabpn1l*$^{-/-}$ females were examined. Error bars indicate SD. (D) Representative images of the embryos at each stage are shown.

The phenotype of developmental arrest at the 2-cell stage has been reported in several studies, and most of them were caused by mutations in Subcortical maternal complex (SCMC) components (*Nlrp2*, *Nlrp5*, *Khdc3*, *Padi6*, *Tle6*, *Ooep*, *Uhrf1*, and *Zar1*). SCMC members have the potential to establish genomic imprints and maintain postzygotic methylation [24–26]. The lack of human SCMC members causes embryonic developmental arrest [27], pregnancy loss, imprinting disorders in offspring [28], and hydatidiform moles [25]. *Pabpn1l*$^{-/-}$ females show infertility owing to early embryonic arrest, implicating PABPN1L in the regulation of SCMC. However, in the RNA sequence data, the RNA expression levels of most of the SCMC members in KO oocytes had expression patterns similar to those in Het oocytes. In agreement with a Zhao's study, it is important to decrease maternal factors before fertilization is completed. In fact, our rescue experiment, in which mRNA was injected at the GV stage partially rescued *the Pabpn1l* KO phenotype but not at the zygote stage. This suggests that the presence of PABPN1L during the GV/MII stage is critical for its function. We found that the expression level of *Khdc3* was 13 times higher in *Pabpn1l* KO-MII oocytes than that in Het-MII oocytes. The main cause of embryonic arrest in *Pabpn1l* KO mice is mRNA accumulation. However, it has been reported that mutations in the *KHDC3L* (ortholog of mouse *Khdc3*) in humans results in DNA methylation disorders and recurrent hydatidiform moles [26], and how the overexpression of *KHDC3L* affects fertility is unclear. It would be interesting to study whether overexpression of this gene during the MII stage is related to developmental arrest at an early embryonic stage. This aspect will be investigated in future studies.

BTG4 recruits the catalytic subunit of CCR4-NOT deadenylase in maturing oocytes and promotes mRNA degradation [29]. Zhao *et al*. revealed that PABPN1L functions in maternal mRNA decay as

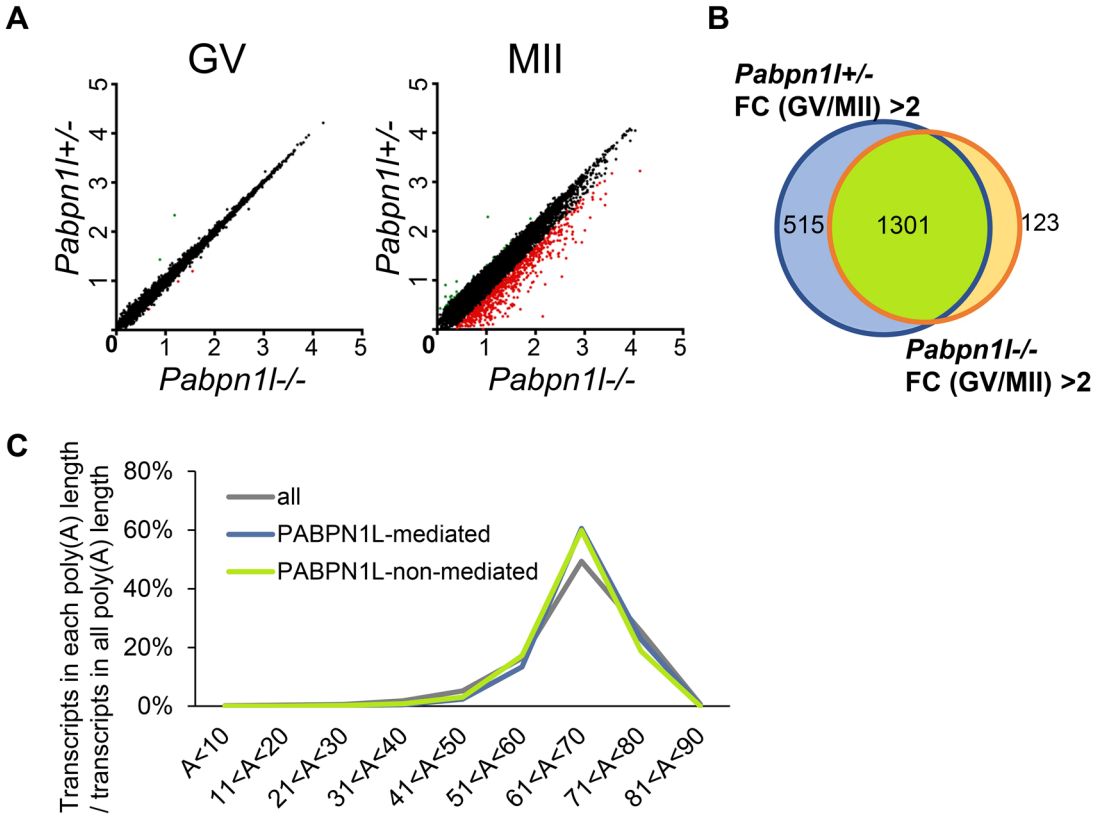

Fig. 3. RNA sequencing analysis of GV and MII oocytes. (A) Scatter plot comparing the transcripts in the oocytes derived from *Pabpn1l*$^{+/-}$ and *Pabpn1l*$^{-/-}$ females at GV and MII stage. These oocytes were cited as Het and KO oocytes, respectively. Transcripts that increased or decreased by more than 2-fold in KO oocytes are shown in red or blue dots, respectively. Het-GV and Het-MII oocytes were considered as controls. Het: heterozygous knockout. KO: homozygous knockout. (B) Venn diagram showing the overlap of transcripts that degraded by more than 2-fold in MII oocytes compared to that in GV oocytes. (C) Frequency of poly(A) tail length of degraded transcripts. All: 12,411 transcripts expressed in the GV oocytes. PABPN1L-dependent: 515 transcripts determined in panel B. PABPN1L-independent: 1,301 transcripts determined in panel B.

a scaffold for BTG4 and the CCR4-NOT complex [16]. Our RNA sequencing data strongly support this theory. However, our RNA sequencing data revealed 1,301 genes with decreased expression levels during the GV/MII transition, regardless of PABPN1L presence. Therefore, another mRNA decay pathway independent of PABPN1L may exist. To determine how PABPN1L targets/recognizes mRNAs, we analyzed the poly(A) lengths of the genes that decreased in PABPN1L-dependent manner (Fig. 3C). No differences were detected in poly(A) length between PABPN1L mediated/non-mediated genes at the GV stage, suggesting that PABPN1L does not prefer poly(A) length for binding. In addition to the poly(A) length analysis, we searched for consensus sequences in transcripts that were degraded in a PABPN1L-dependent manner. However, we did not identify any consensus sequences. Three-dimensional structural analysis may help us understand the selectivity.

Since the embryonic arrest at the 2-cell stage was rescued when *Pabpn1l* mRNA was exogenously expressed in KO-GV oocytes, it is considered that mRNA degradation via PABPN1L through GV/MII maturation is critical for development. PABPC1 facilitates mRNA degradation by recruiting the CNOT complex [6, 7], and PABPC1 only appears after fertilization. Thus, we hypothesized that PABPC1 compensates for the function of PABPN1 when expressed at the GV/MII stage. Contrary to our hypothesis, the exogenous expression of *Pabpc1* from the GV stage did not rescue the 2-cell arrest observed in *Pabpn1l* KO oocytes (Supplementary Fig. 5). These results could be explained by that PABPN1L recruits BTG4/CNOT complex whereas PABPC1 recruits the TOB/CNOT complex and/or a unique function of PABPN1L.

Zhao *et al*. reported the mRNA expression patterns in oocytes and zygotes are derived from *Pabpn1l*$^{-/-}$ females [16]. mRNA expression levels were compared between GV oocytes and zygotes, whereas GV and MII oocytes were used in this study. A comparison of these data enabled us to identify the transcripts that initially decreased in a PABPN1L-dependent manner in MII oocytes and zygotes. This study shows that the exogenous expression of *Pabpn1l* in KO-GV oocytes could rescue developmental defects. This approach opens up the possibility of infertility treatments that cannot be saved by intracytoplasmic sperm injection (ICSI) or IVF.

Our results indicated that PABPN1L is essential for female fertility in mice because it facilitates mRNA decay during GV to MII maturation and subsequent embryonic development. Genome editing and transgenic/mRNA complementation assays will shed light on the oocyte/zygote transition stage, which is an important event for the next generation. Because PABPN1L is conserved among mammals, including humans, it may be a novel candidate for the treatment of female infertility.

Conflict of interests: The authors declare that there are no conflicts of interests.

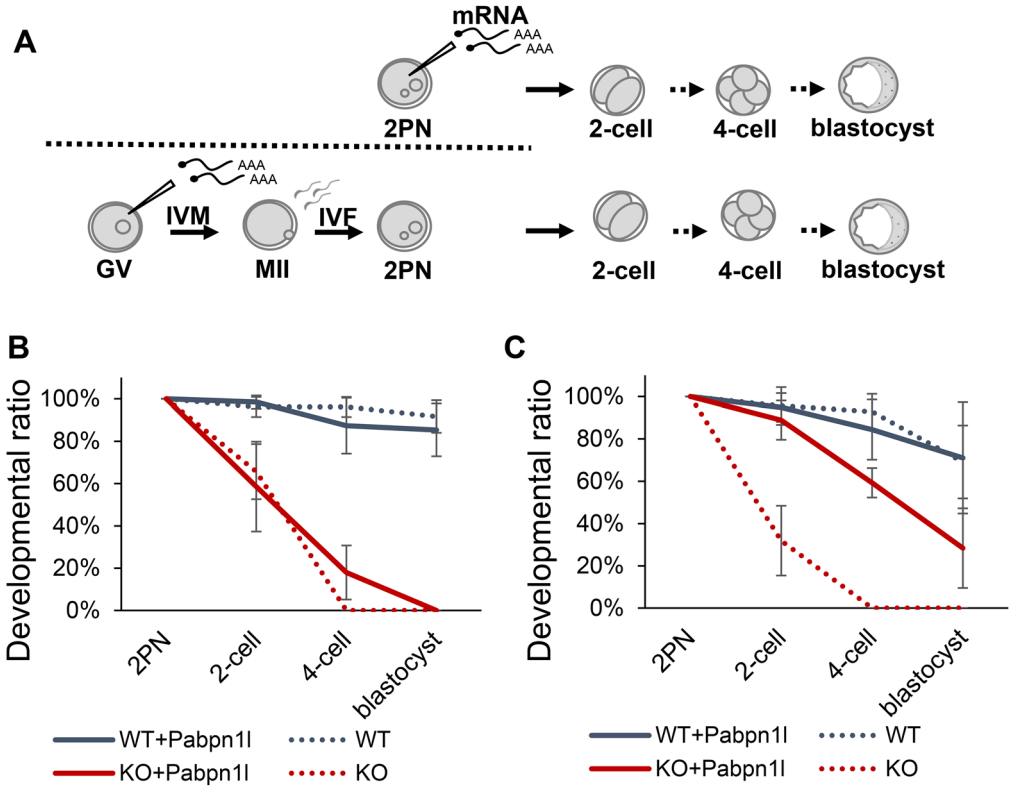

Fig. 4. PABPN1L functional period in oocytes and embryos. (A) Experimental scheme of mRNA injection. *Pabpn1l*-mRNA and EGFP-mRNA were injected into 2PN embryos (upper) or GV oocytes (lower). Then, embryo development was observed until the blastocyst stage. (B) Developmental ratio of mRNA injection at 2PN embryos. The number of 2-cell embryos, 4-cell embryos, and blastocysts was divided by the number of 2PN embryos. We examined 90, 56, 100, 65 embryos in WT embryos injected, intact WT embryos, injected embryos derived from *Pabpn1l*$^{-/-}$ females, and intact embryos derived from *Pabpn1l*$^{-/-}$ females, respectively. KO; knockout. Technical replicates = 5. Dotted line: without injection of mRNAs. Solid lines: with injection of mRNAs. Error bars indicate SD. (C) Developmental ratio of mRNA injection at GV oocytes. The number of 2-cell embryos, 4-cell embryos, and blastocysts was divided by the number of 2PN embryos. We examined 40, 110, 55, 115 oocytes in injected WT oocytes, intact WT oocytes, injected KO oocytes, and intact KO oocytes, respectively. KO; knockout. Technical replicates = 5. Dotted line: without injection of mRNAs. Solid lines: with injection of mRNAs. Error bars indicate SD.

Acknowledgments

We acknowledge the NGS core facility of the Genome Information Research Center at the Research Institute for Microbial Diseases of Osaka University for their support in RNA sequencing and data analysis and Biotechnology Research and Development (nonprofit organization) for their support in generating genetically modified mice. This work was supported by the Ministry of Education, Culture, Sports, Science and Technology (MEXT)/Japan Society for the Promotion of Science (JSPS) KAKENHI grants (JP19H05750 to M. I. and 21K15009 to C.E.).

References

1. **Gagliardi D, Dziembowski A.** 5′ and 3′ modifications controlling RNA degradation: from safeguards to executioners. *Philos Trans R Soc Lond B Biol Sci* 2018; **373**: 1–5. [Medline] [CrossRef]
2. **Legrand JMD, Hobbs RM.** RNA processing in the male germline: Mechanisms and implications for fertility. *Semin Cell Dev Biol* 2018; **79**: 80–91. [Medline] [CrossRef]
3. **Preiss T, Hentze MW.** From factors to mechanisms: translation and translational control in eukaryotes. *Curr Opin Genet Dev* 1999; **9**: 515–521. [Medline] [CrossRef]
4. **Sachs A.** 10 Physical and functional interactions between the mRNA cap structure and the poly (A) tail. *Translational Control of Gene Expression* 2000; **39**: 447–465. [CrossRef]
5. **Banerjee A, Apponi LH, Pavlath GK, Corbett AH.** PABPN1: molecular function and muscle disease. *FEBS J* 2013; **280**: 4230–4250. [Medline] [CrossRef]
6. **Bresson S, Tollervey D.** Tailing off: PABP and CNOT generate cycles of mRNA deadenylation. *Mol Cell* 2018; **70**: 987–988. [Medline] [CrossRef]
7. **Yi H, Park J, Ha M, Lim J, Chang H, Kim VN.** PABP cooperates with the CCR4-NOT complex to promote mRNA deadenylation and block precocious decay. *Mol Cell* 2018; **70**: 1081–1088.e5. [Medline] [CrossRef]
8. **De La Fuente R.** Chromatin modifications in the germinal vesicle (GV) of mammalian oocytes. *Dev Biol* 2006; **292**: 1–12. [Medline] [CrossRef]
9. **Christou-Kent M, Dhellemmes M, Lambert E, Ray PF, Arnoult C.** Diversity of RNA-binding proteins modulating post-transcriptional regulation of protein expression in the maturing mammalian oocyte. *Cells* 2020; **9**: 662. [Medline] [CrossRef]
10. **Schier AF.** The maternal-zygotic transition: death and birth of RNAs. *Science* 2007; **316**: 406–407. [Medline] [CrossRef]
11. **Tadros W, Lipshitz HD.** The maternal-to-zygotic transition: a play in two acts. *Development* 2009; **136**: 3033–3042. [Medline] [CrossRef]
12. **Yang Y, Zhou C, Wang Y, Liu W, Liu C, Wang L, Liu Y, Shang Y, Li M, Zhou S, Wang Y, Zeng W, Zhou J, Huo R, Li W.** The E3 ubiquitin ligase RNF114 and TAB1 degradation are required for maternal-to-zygotic transition. *EMBO Rep* 2017; **18**: 205–216. [Medline] [CrossRef]
13. **Sha QQ, Zheng W, Wu YW, Li S, Guo L, Zhang S, Lin G, Ou XH, Fan HY.** Dynamics and clinical relevance of maternal mRNA clearance during the oocyte-to-embryo transition in humans. *Nat Commun* 2020; **11**: 4917. [Medline] [CrossRef]
14. **Guzeloglu-Kayisli O, Lalioti MD, Aydiner F, Sasson I, Ilbay O, Sakkas D, Lowther KM, Mehlmann LM, Seli E.** Embryonic poly(A)-binding protein (EPAB) is required for oocyte maturation and female fertility in mice. *Biochem J* 2012; **446**: 47–58. [Medline] [CrossRef]
15. **Good PJ, Abler L, Herring D, Sheets MD.** Xenopus embryonic poly(A) binding protein 2 (ePABP2) defines a new family of cytoplasmic poly(A) binding proteins expressed during the early stages of vertebrate development. *Genesis* 2004; **38**: 166–175. [Medline] [CrossRef]
16. **Zhao LW, Zhu YZ, Chen H, Wu YW, Pi SB, Chen L, Shen L, Fan HY.** PABPN1L mediates cytoplasmic mRNA decay as a placeholder during the maternal-to-zygotic transition. *EMBO Rep* 2020; **21**: e49956. [Medline] [CrossRef]
17. **Naito Y, Hino K, Bono H, Ui-Tei K.** CRISPRdirect: software for designing CRISPR/Cas guide RNA with reduced off-target sites. *Bioinformatics* 2015; **31**: 1120–1123. [Medline]

[CrossRef]

18. **Mashiko D, Fujihara Y, Satouh Y, Miyata H, Isotani A, Ikawa M.** Generation of mutant mice by pronuclear injection of circular plasmid expressing Cas9 and single guided RNA. *Sci Rep* 2013; **3**: 3355. [Medline] [CrossRef]
19. **Muro Y, Hasuwa H, Isotani A, Miyata H, Yamagata K, Ikawa M, Yanagimachi R, Okabe M.** Behavior of mouse spermatozoa in the female reproductive tract from soon after mating to the beginning of fertilization. *Biol Reprod* 2016; **94**: 80. [Medline] [CrossRef]
20. **Toyoda Y, Yokoyama M, Hosi T.** Studies on the fertilization of mouse eggs in vitro. II. Effects of in vitro preincubation of spermatozoa on time of sperm penetration of mouse eggs in vitro. *Japanese Journal of Animal Reproduction* 1971; **16**: 152–157.
21. **Ho Y, Wigglesworth K, Eppig JJ, Schultz RM.** Preimplantation development of mouse embryos in KSOM: augmentation by amino acids and analysis of gene expression. *Mol Reprod Dev* 1995; **41**: 232–238. [Medline] [CrossRef]
22. **Morgan M, Much C, DiGiacomo M, Azzi C, Ivanova I, Vitsios DM, Pistolic J, Collier P, Moreira PN, Benes V, Enright AJ, O'Carroll D.** mRNA 3′ uridylation and poly(A) tail length sculpt the mammalian maternal transcriptome. *Nature* 2017; **548**: 347–351. [Medline] [CrossRef]
23. **Hayashi K, Hikabe O, Obata Y, Hirao Y.** Reconstitution of mouse oogenesis in a dish from pluripotent stem cells. *Nat Protoc* 2017; **12**: 1733–1744. [Medline] [CrossRef]
24. **Monk D, Sanchez-Delgado M, Fisher R.** NLRPs, the subcortical maternal complex and genomic imprinting. *Reproduction* 2017; **154**: R161–R170. [Medline] [CrossRef]
25. **Elbracht M, Mackay D, Begemann M, Kagan KO, Eggermann T.** Disturbed genomic imprinting and its relevance for human reproduction: causes and clinical consequences. *Hum Reprod Update* 2020; **26**: 197–213. [Medline] [CrossRef]
26. **Demond H, Anvar Z, Jahromi BN, Sparago A, Verma A, Davari M, Calzari L, Russo S, Jahromi MA, Monk D, Andrews S, Riccio A, Kelsey G.** A KHDC3L mutation resulting in recurrent hydatidiform mole causes genome-wide DNA methylation loss in oocytes and persistent imprinting defects post-fertilisation. *Genome Med* 2019; **11**: 84. [Medline] [CrossRef]
27. **Wu X, Viveiros MM, Eppig JJ, Bai Y, Fitzpatrick SL, Matzuk MM.** Zygote arrest 1 (Zar1) is a novel maternal-effect gene critical for the oocyte-to-embryo transition. *Nat Genet* 2003; **33**: 187–191. [Medline] [CrossRef]
28. **Begemann M, Rezwan FI, Beygo J, Docherty LE, Kolarova J, Schroeder C, Buiting K, Chokkalingam K, Degenhardt F, Wakeling EL, Kleinle S, González Fassrainer D, Oehl-Jaschkowitz B, Turner CLS, Patalan M, Gizewska M, Binder G, Bich Ngoc CT, Chi Dung V, Mehta SG, Baynam G, Hamilton-Shield JP, Aljareh S, Lokulo-Sodipe O, Horton R, Siebert R, Elbracht M, Temple IK, Eggermann T, Mackay DJG.** Maternal variants in *NLRP* and other maternal effect proteins are associated with multilocus imprinting disturbance in offspring. *J Med Genet* 2018; **55**: 497–504. [Medline] [CrossRef]
29. **Yu C, Ji SY, Sha QQ, Dang Y, Zhou JJ, Zhang YL, Liu Y, Wang ZW, Hu B, Sun QY, Sun SC, Tang F, Fan HY.** BTG4 is a meiotic cell cycle-coupled maternal-zygotic-transition licensing factor in oocytes. *Nat Struct Mol Biol* 2016; **23**: 387–394. [Medline] [CrossRef]
30. **Kaneko T, Mashimo T.** Simple genome editing of rodent intact embryos by electroporation. *PLoS One* 2015; **10**: e0142755. [Medline] [CrossRef]